Numerical simulation of High Intensity Focused Ultrasound (HIFU) using a fully compressible multiscale model

Aswin Gnanaskandan*; Chao-Tsung Hsiao; Georges Chahine

DYNAFLOW, INC., MD, USA

Abstract

A fully compressible multiscale model for simulation of bubble enhanced High Intensity Focused Ultrasound (HIFU) is presented. The non-linear ultrasound field is modeled using compressible Navier-Stokes equations on a fixed grid, while the microbubbles are tracked as discrete singularities in a Lagrangian fashion. These two models are two-way coupled to each other such that both the acoustic field and the bubbles influence each other. The energy absorbed by the medium locally due to the focused ultrasound and bubble dynamics is then used to compute the temperature rise in the focal and surrounding regions by solving a heat transfer equation over the insonation time period. We first simulate the HIFU field without microbubbles and characterize the pressure and temperature fields and compare against available experiments. Experimental validation in the presence of microbubbles is then carried out to demonstrate the accuracy of the model. We then study the effect of the microbubbles on altering the temperature rise obtained in the focal region.

Keywords: HIFU; Euler-Lagrange method; microbubbles

Introduction

High Intensity Focused Ultrasound (HIFU) uses the focused energy of sound waves to elevate temperature locally, causing thermal ablation of tissues. For deep seated cancers, higher intensity sound waves are required to reach the target area [1]. However, this may cause unwanted tissue damage outside of the targeted region. A major impediment with the current use of HIFU technique to efficiently treat deep seated cancer is the long treatment time whilst using higher intensity for deeper penetration. In order to reduce undesirable damage of surrounding tissues, the resting time for cooling in the pre-focal regions has to be increased. It is therefore desirable to obtain higher temperature elevations at the focal region while still using moderate intensity levels (100 – 1000 W/cm^2) [2]. Introducing microbubbles in the form of contrast agents has been shown to increase temperature levels in both *in vitro* [3], [4] and *in vivo* experiments [5], [6]. However the exact mechanism of how the microbubbles contribute to the heat increase has only been speculative due to the difficulty in both experimental measurements and computational modeling.

The physical mechanism of heat enhancement through bubbles is thought to be primarily from three mechanism viz. acoustic emission, viscous dissipation, and thermal exchange [7]. Acoustic damping of the bubble oscillations arises because the bubble radiates acoustic energy and becomes important primarily when the bubble undergoes inertial oscillations. Viscous damping arises primarily from viscous dissipation in the relatively thin layer of host medium surrounding the bubble that moves during the bubble oscillations. The dissipation is directly proportional to the bubble interfacial velocity and the shear viscosity of the host medium. Thermal damping arises from the heat flow into the bubble during its expansion phase and out of the bubble during its collapse phase. The net amount of such heat flow for a particular bubble oscillation depends on the oscillation amplitude, which, in turn, is a strong function of the insonation pressure, frequency, and equilibrium bubble size. The relative contribution of these terms, as explained above, depends on a variety of factors and numerical simulations can shed light on the importance of these terms, if properly modeled. The main objective of this work is to develop a numerical model to simulate HIFU in the presence of microbubbles, verify its validity and apply it to understand the effect of bubbles on heat enhancement.

Physical model and numerical method

A fully compressible Euler-Lagrange model is employed in this study. The background acoustic and flow field is solved using the compressible Navier-Stokes equations on a fixed grid, while the presence of microbubbles are modeled by solving Keller-Herring equation given by,

*Corresponding Author, Aswin Gnanaskandan: aswin@dynaflow-inc.com

$$(1-\frac{\dot{R}}{c})R\ddot{R}+\frac{3}{2}(1-\frac{\dot{R}}{3c})\dot{R}^2=\frac{1}{\rho}(1+\frac{\dot{R}}{c}+\frac{R}{c}\frac{d}{dt})\left[p_v+p_g-p_l-\frac{2\gamma}{R}-4\mu\frac{\dot{R}}{R}-\frac{4}{3}G\left[1-\left(\frac{R_0}{R}\right)^3\right]\right]+\frac{(\mathbf{u}_l-\mathbf{u}_b)^2}{4}. \quad (1)$$

Here, R is the radius of the bubble, $\dot{R}$ is the bubble interface velocity, ρ, c and μ are the density, sound speed and viscosity of the surrounding medium. p_v, p_g are the vapor and gas pressure inside the bubble and p_l is the liquid pressure driving the bubble dynamics. γ is the surface tension and G is the shear elasticity of the medium. We account for the motion of the bubbles by solving a motion equation, which accounts for effect of the slip velocity between the bubble of velocity $\mathbf{u}_b$ and the liquid of velocity $\mathbf{u}_l$.

$$\frac{d\mathbf{u}_b}{dt}=-\frac{3}{\rho_l}\nabla p+\frac{3}{4}\frac{C_D}{R}(\mathbf{u}_l-\mathbf{u}_b)\mathbf{u}_l-\mathbf{u}_b+\frac{3\dot{R}}{R}(\mathbf{u}_l-\mathbf{u}_b), \quad (2)$$

where C_D is a drag coefficient and the last term is a Bjerknes force term due to coupling between bubble volume oscillations and bubble motion.

The ultrasound source is modelled as an imposed pressure distribution with phasing on the inlet boundary (z=0) [8],

$$p(z=0,r,t)=p_0\sin\left[2\pi f_0\left(t+\frac{r^2}{2cF}\right)\right], \quad (3)$$

where p_0 and f_0 are the amplitude and frequency of the ultrasound and r and F are the radius and focal length of the transducer. Since the actual insonation time is of the order of 1 s, orders of magnitude higher than the acoustic field CFD computation, we used a decoupled approach [2], [9], [10], where after solving the dynamic equations, we separately solve a heat transfer equation,

$$\rho C_p\frac{\partial T}{\partial \tau}=K\nabla^2 T+q_{US,AC}+q_{VIS}+q_{THER}, \quad (4)$$

where ρ, C_p and K are the density, specific heat and thermal conductivity of the medium, T is the temperature and τ is time. The heat sources, q_*, in this equation are due to the viscous dissipation of ultrasound and acoustics, and due to viscous and thermal damping of the bubbles. The heat source due to ultrasound absorption and acoustic damping of the bubble is given by

$$q_{US,AC}=\mu_b\varepsilon_{kk}^2+2\mu\left(\varepsilon_{ij}-\frac{1}{3}\varepsilon_{kk}\delta_{ij}\right)^2, \quad (5)$$

where μ and μ_b are the shear and bulk viscosity of the medium and $\boldsymbol{\varepsilon}$ is the strain rate tensor. The heat addition due to the viscous damping of the bubble in a given control volume is given by

$$q_{VIS}=\sum_{j=1}^{N_i}\frac{q_{vis}^b f_{i,j}}{\sum_{k=1}^{Ncells}V_k^{cell}f_{k,j}}, \qquad q_{vis}^b=\left(4\pi R_b^2\right).\left(4\mu\frac{\dot{R}_b^2}{R_b}\right), \quad (6)$$

where $f_{i,j}$ is the smoothing kernel [11], V_k is the volume of the control volume. The heat addition due to thermal damping of bubbles is not modelled in this study and will be considered in future studies.

For closing the Navier Stokes equations, a stiffened gas equation of state is used. For details regarding the numerical method for the Eulerian and Lagrangian approached refer to [12] and [11]. All the results in this study have been obtained using axisymmetric simulations for the Eulerian phase, while bubble distributions were fully 3D.

Results and discussion

The acoustic calculation is first verified by computing a focused ultrasound field in water in both linear and non-linear regimes. For the linear regime, we compare with the experiments in [13], where a 1.1 MHz transducer of radius 35 mm and focal length 60 mm is used with a source pressure amplitude P_a = 0.01 MPa. We compare the focal scan data obtained along the axis with the numerical results in Figure 1(a). The focal scan showing the magnitude of pressure

*Corresponding Author, Aswin Gnanaskandan: aswin@dynaflow-inc.com

peaks along the axis agrees well with the experiment indicating that the area in which the ultrasound is focused is predicted properly. In Figure 1(b), we compare the pressure history obtained at the focal point for a 2.2 MHz transducer of 20 mm radius and 44 mm focal length at a source pressure of 0.29 MPa corresponding to the experiments in [8]. At this source pressure, non-linear steepening of the acoustic waves results in a shock wave at the focus, which is captured well by the numerical simulations.

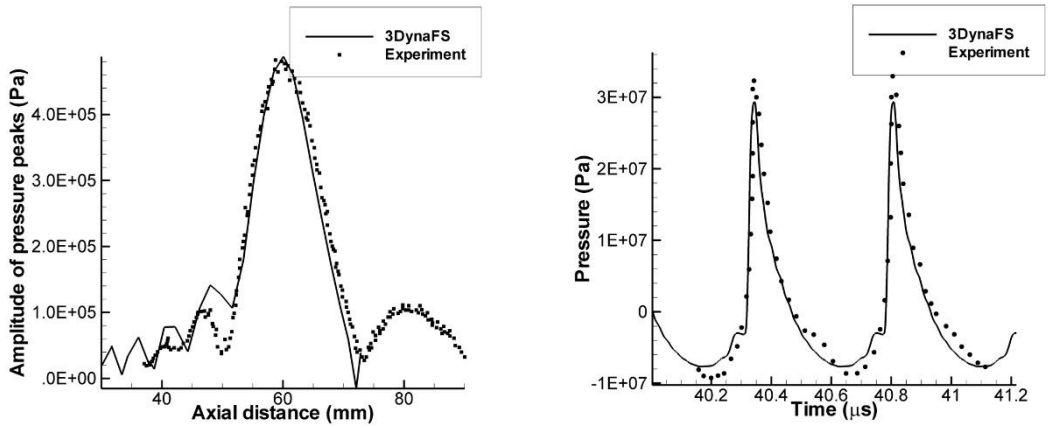

Figure 1: Characterization of the acoustic field in linear and non-linear regime in water. (a) Comparison of focal scan data along the axis with the experiments in [13] for 1 MHz transducer with source pressure Pa = 0.01 MPa, linear regime. (b) Comparison of time history of pressure at the focus with the experiments in [8] for 2.2 MHz transducer with source Pa = 0.28 MPa, non-linear regime. Profile shows non-linear steepening of acoustic waves.

Next, we validate the numerical method for a HIFU procedure in a phantom tissue without introducing any bubbles. The experiments are from [10], where a phantom tissue made of Agar is subjected to focused ultrasound from a 1.1 MHz transducer of radius 35 mm and focal length 60mm. The peak rarefaction at the focus is 1.1 MPa. The considered properties of the Agar are ρ=1,044 Kg/m^3, μ = 0.3 Pa.s and shear elasticity is neglected. The focused ultrasound field is depicted in Figure 2(a), where the acoustic waves are seen to focus at the geometric focus. The heat absorbed by the phantom tissue is obtained as a time averaged quantity over 0.01 ms and is further used as source term in the heat equation. The time averaged contours of heat release, depicted in Figure 2(b), shows heat concentration around the focal region. Note that the contours in Figure 2(b) are in logarithmic scale for clarity and that the highest value around the focus is at least an order of magnitude higher than that in the pre and post focal regions.

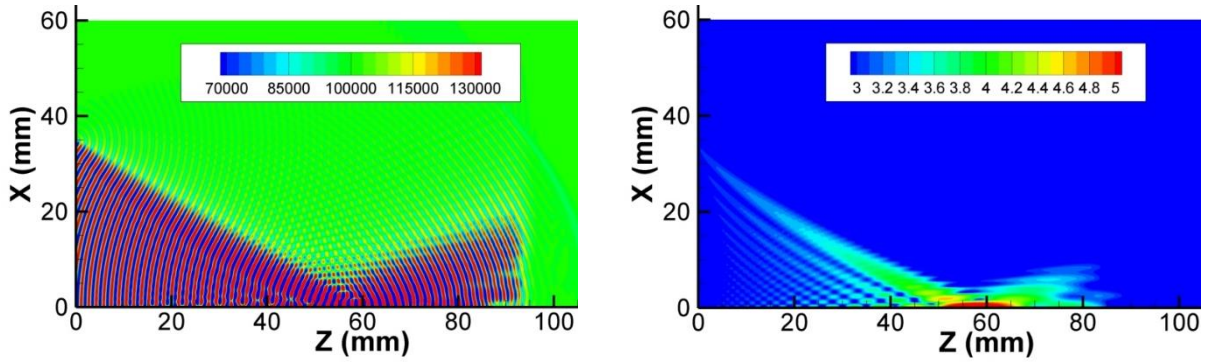

Figure 2: (a) Instantaneous contours of pressure showing focusing of the wave at z = 60 mm. (b) Contours of the time averaged (for 0.01ms) heat release computed from the hydrodynamic field. Logarithm of heat release is plotted for clarity. The simulations are based on the experiments in [10] with a 1 MHz transducer.

Comparison of the temperature history between simulation and experiments at the focus and at one off-focus location is depicted in Figure 3. The ultrasound source is on for 1s followed by a cooling time of 4 s. The simulations results show good agreement with the experiments indicating the accuracy of the physical model and the numerical method in simulating HIFU flow field.

*Corresponding Author, Aswin Gnanaskandan: aswin@dynaflow-inc.com

Finally, the model is applied to study HIFU in the presence of microbubbles. The simulations correspond to the *invitro* experiments in [3], where a 2.2 MHz transducer of radius 20 mm and focal length of 40 mm is used to insonate a phantom tissue made of Polyacrylamide gel. The density of the gel is 1,060 Kg/m^3, the viscosity is 0.01 Pa.s, and the shear elasticity is 0.1 MPa. Bubbles of radius 1.3 μm are distributed uniformly in a cylindrical volume of length 10 mm and diameter 10 mm centered at the geometric focus (z = 40 mm). Acoustic calculations are carried out for 0.1 ms and the time averaged source terms for the heat equation are computed over 0.01 ms. The heat equation is then solved for 60 s with the source terms. Figure 4(a) shows the instantaneous pressure contours in the presence of bubbles. Two different void fractions $\alpha = 1x10^{-4}$ and $1x10^{-5}$ (shown in Figure 4 (a)) are used. The scattering of pressure waves due to the bubbles is evident; the bubbles also attenuate the ultrasound waves before they reach the focus. The temperature history obtained at several locations near the geometric focus are compared to the experimental data [3] in Figure 4 (b). Since the location of the temperature measurement in the experiment is not known, we only compare qualitatively the temperature profile at a few locations around the geometric focus. Although the quantitative agreement is not satisfactory, the simulations reproduce the qualitative trend in the experiment.

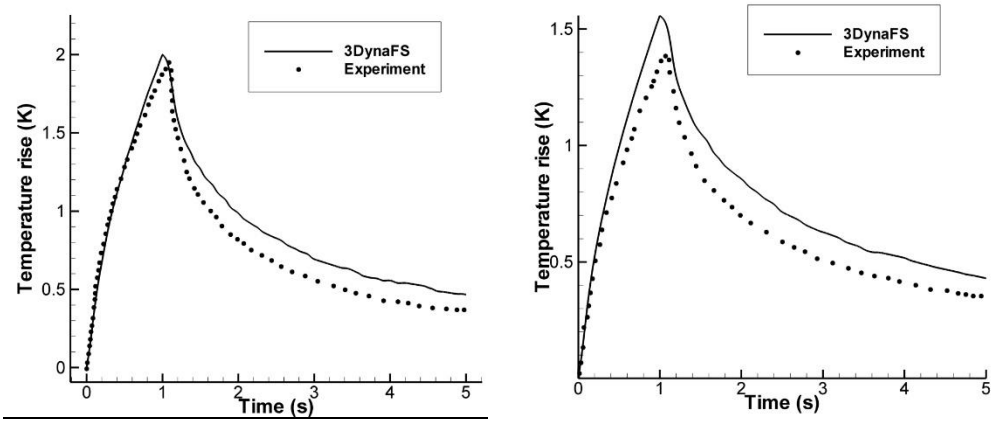

Figure 3: Comparison of the temperature history obtained from HIFU simulations in phantom tissue without bubbles with experiments in [10] for 1s of insonation followed by cooling for 4s. (a) At the focal point, z = 60mm. (b) At a point away from the focus, at x = 0.1 mm and z = 60 mm.

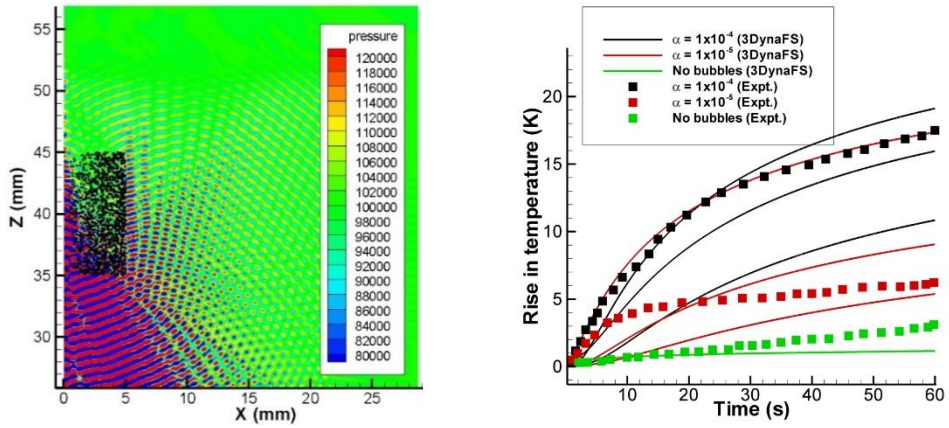

Figure 4: (a) Instantaneous pressure contours from HIFU simulations in phantom tissue with bubbles. The bubbles are distributed uniformly inside a cylinder of length 10mm and diameter 10 mm centered at the geometric focus as in the experiments in [3]. The bubble sizes have been magnified by 125 times to enhance visibility. (b) Comparison of the temperature history with the experimental data at a few locations in the focal region.

It is evident that the presence of bubbles leads to an increase in temperature. However, it is known that the presence of bubbles can attenuate the ultrasound propagation and hence it is necessary to ascertain whether the increased temperature is obtained in the desired focal region or not. Figure 5(a) shows the distribution of temperature along the axis for different void fractions. It is evident that the presence of bubbles leads to an increased temperature; however,

*Corresponding Author, Aswin Gnanaskandan: aswin@dynaflow-inc.com

the location of the peak temperature shifts to the geometric pre-focal region as the void fraction is increased. The attenuation is larger for larger void fractions, which also results in the shifting of the focal region towards the transducer. Figure 5(b) shows the effect of the localization of bubbles for $\alpha = 1x10^{-5}$. The results with the bubbles distributed in a fictitious cylinder of length 5 mm and diameter 5 mm, are compared with the experimental configuration of 10 mm x 10 mm cylinder. With the 5 mm cylinder, the bubbles are present only near the focus, thereby the attenuation of the ultrasound by the bubbles is reduced leading to a higher temperature increase.

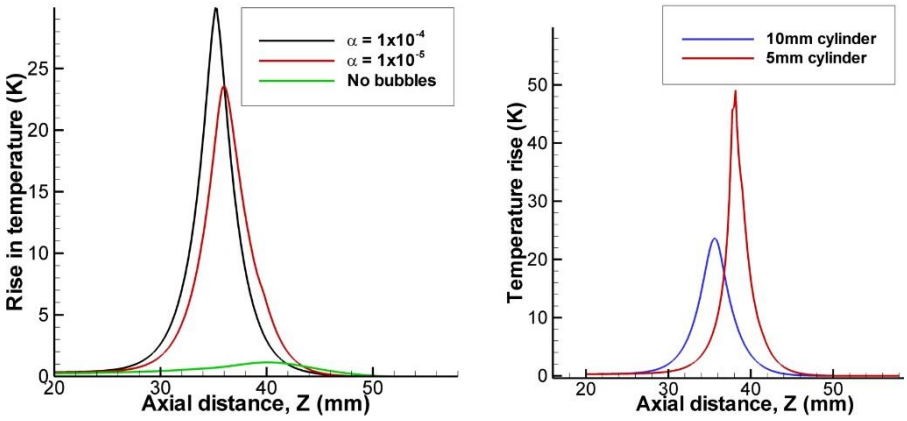

Figure 5: (a) Distribution of the temperature along the Z-axis obtained from the 3DYNAFS-COMP© / 3DYNAFS-DSM© coupled simulations for different void fractions. (b) Effect of bubble localization around the focus (z = 40 mm) on the temperature distribution along the Z-axis.

The individual contributions of the heat source due to ultrasound absorption, acoustic damping and viscous damping of the bubbles are plotted Figure 6(a) and (b). The heat due to ultrasound absorption and acoustic damping are combined as a single term. The viscous damping contribution is only at the location of the bubbles and its magnitude is approximately 2 orders of magnitude higher than the contribution of the acoustic dissipation to heat release. Both contours are represented using their respective logarithmic values for clarity. This demonstrates that for the current simulations, viscous damping of the bubbles plays the main role in adding heat locally in the vicinity of the bubbles. However, due to the long insonation time (60s), the heat diffuses away from the bubbles.

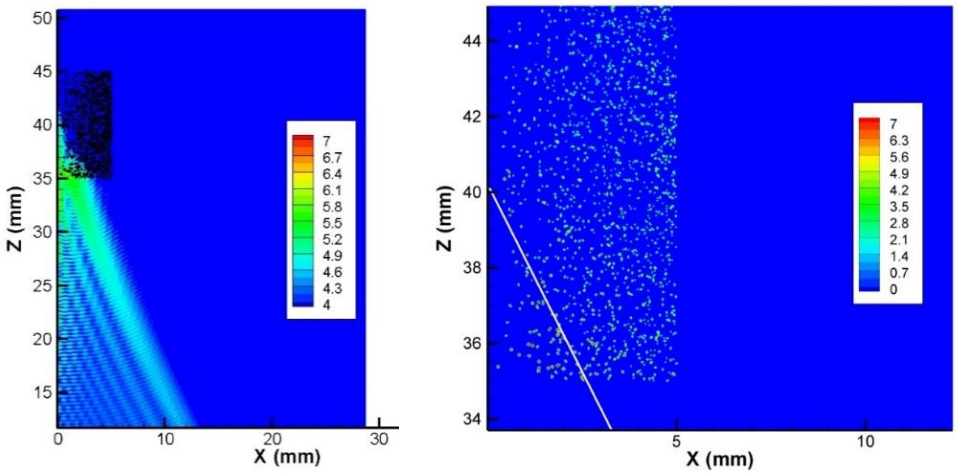

Figure 6: (a) Time averaged contours of heat source due to the absorption of ultrasound by the medium and acoustic damping of bubbles. (b) Time averaged contours of heat released due to the viscous damping of bubble oscillations by the surrounding medium.

Conclusion

A fully compressible multiscale numerical model is presented for the simulation of a bubble enhanced HIFU field. The non-linear acoustic field modeled in an Eulerian framework is coupled to a bubble dynamics solver, where the

*Corresponding Author, Aswin Gnanaskandan: aswin@dynaflow-inc.com

individual bubbles are tracked in a Lagrangian fashion. The method is first validated using *in vitro* experiments in the absence of microbubbles. Good agreement for temperature profile is obtained in and around the focal region. The method is then applied to HIFU simulation in the presence of microbubbles. Relatively good agreement of the temperature profiles around the focal region is obtained for two different void fractions. The effect of localization of bubbles is then demonstrated by concentrating the bubbles close to the focal location, which results in higher temperature increase due to reduced attenuation of the ultrasound.

Acknowledgements

We gratefully acknowledge the support from NIH under SBIR Grant No. 1R43CA213866-01A1

References

[1] J. E. Kennedy *et al.*, "High-intensity focused ultrasound for the treatment of liver tumours.," *Ultrasonics*, vol. 42, no. 1–9, pp. 931–5, Apr. 2004.

[2] P. Hariharan, M. R. Myers, and R. K. Banerjee, "HIFU procedures at moderate intensities—effect of large blood vessels," *Phys. Med. Biol.*, vol. 52, no. 12, pp. 3493–3513, Jul. 2007.

[3] K. Kajiyama, K. Yoshinaka, S. Takagi, and Y. Matsumoto, "Micro-bubble enhanced HIFU," *Phys. Procedia*, vol. 3, no. 1, pp. 305–314, Jan. 2010.

[4] D. Razansky, P. D. Einziger, and D. R. Adam, "Enhanced heat deposition using ultrasound contrast agent - modeling and experimental observations," *IEEE Trans. Ultrason. Ferroelectr. Freq. Control*, vol. 53, no. 1, pp. 137–147, Jan. 2006.

[5] Y. Kaneko *et al.*, "Use of a microbubble agent to increase the effects of high intensity focused ultrasound on liver tissue," *Eur. Radiol.*, vol. 15, no. 7, pp. 1415–1420, Jul. 2005.

[6] D. J. Chung, S. H. Cho, J. M. Lee, and S.-T. Hahn, "Effect of microbubble contrast agent during high intensity focused ultrasound ablation on rabbit liver in vivo," *Eur. J. Radiol.*, vol. 81, no. 4, pp. e519–e523, Apr. 2012.

[7] R. G. Holt and R. A. Roy, "Measurements of bubble-enhanced heating from focused, MHz-frequency ultrasound in a tissue-mimicking material," *Ultrasound Med. Biol.*, vol. 27, pp. 1399–1412, 2001.

[8] M. S. Canney, M. R. Bailey, L. A. Crum, V. A. Khokhlova, and O. A. Sapozhnikov, "Acoustic characterization of high intensity focused ultrasound fields: a combined measurement and modeling approach.," *J. Acoust. Soc. Am.*, vol. 124, no. 4, pp. 2406–20, Oct. 2008.

[9] K. Okita, K. Sugiyama, S. Takagi, and Y. Matsumto, "Microbubble behavior in an ultrasound field for high intensity focused ultrasound therapy enhancement," *J. Acoust. Soc. Am.*, vol. 134, no. 2, pp. 1576–1585, Aug. 2013.

[10] J. Huang, R. G. Holt, R. O. Cleveland, and R. A. Roy, "Experimental validation of a tractable numerical model for focused ultrasound heating in flow-through tissue phantoms," *J. Acoust. Soc. Am.*, vol. 116, no. 4, pp. 2451–2458, Oct. 2004.

[11] J. Ma, G. L. Chahine, and C.-T. Hsiao, "Spherical bubble dynamics in a bubbly medium using an Euler–Lagrange model," *Chem. Eng. Sci.*, vol. 128, pp. 64–81, May 2015.

[12] A. Kapahi, C. Hsiao, and G. Chahine, "A multi-material flow solver for high speed compressible flows," *Comput. Fluids*, 2015.

[13] J. Huang, "Heating in Vascular Tissue and Flow-through Tissue Phantoms Induced by Focused Ultrasound," *PhD Thesis*, 2002.

*Corresponding Author, Aswin Gnanaskandan: aswin@dynaflow-inc.com